Interference fit equations for lens cell design using elastomeric lens mountings

Tina M. Valente
Ralph M. Richard, MEMBER SPIE
Optical Sciences Center
University of Arizona
Tucson, Arizona 85721

Abstract. Optical designs often consist of lenses that are mounted in a common lens barrel. For lenses having diameters greater than 20 cm and subject to large temperature differentials and/or shock loading, standard metal retainer ring mountings may not be acceptable. An alternate method for mounting these lenses is to mount each individual lens in its own subcell using an adhesive and then to use an interference or press fit to mount these subcells in the lens barrel. When mounting lenses in this manner, it is necessary to evaluate the stress induced in the glass and the residual difference in the optical path. A closed-form analytical derivation was made for a simple lens mount that relates the allowable magnitude of the interference fit to the stress in the glass. This theoretical expression was then modified using finite element models for use with complex lens designs. Moreover, since lens mountings may require the use of relatively thick layers of flexible elastomer to mount the lenses in their individual cells to prevent large thermal and/or mechanical stresses, the equation for determining the decentration of lenses mounted in circumferential flexible elastomers is also derived. The theoretical expression was used to verify finite element models that then may be used for more complex mounts.

Subject terms: lens mountings; subcell mountings; interference fits; elastomeric mountings; lens cells; lens decentration; optical path differences.

Optical Engineering 33(4), 1223–1228 (April 1994).

1 Introduction

For small optical devices, glass lenses are generally mounted directly into their metal cell and held in position with metal retainer rings. However, optical elements with diameters of 20 cm or greater that are subject to adverse temperature and shock loadings may require an alternative mounting using relatively thick and flexible layers of elastomers to reduce thermal and mechanical stresses in the lenses.

Closed-form analytical equations for simple lens mounting may be derived from the classical theory of elasticity and solid mechanics. These equations, in addition to defining stresses and displacements for simple lens mountings, also provide solutions that may be used to verify finite element modeling techniques that, in turn, can be extended to more complex lens mountings. These finite element models may also be used to generate empirical relationships that, when used with the classical solutions, provide closed-form solutions to complex lens mounting problems. Presented here are derived equations that may be used to predict stresses, strains, and displacements in lenses mounted in a common lens barrel using elastomers and interference or press fits. Comparisons are made between classical and finite element solutions that provide a high confidence level for the complex lens mounts.

Paper 09043 received Apr. 12, 1993; revised manuscript received Oct. 6, 1993; accepted for publication Oct. 24, 1993.

2 Interference Fit Equations

The equations that give the displacements and stresses between and interior to cylinders that are force-fitted are derived from compatibility and equilibrium considerations of the theory of elasticity. Shown in Fig. 1 is a cross section of a short cylinder of length l_i that is force-fitted into a longer cylinder of length l_o. For the case where l_o is equal to l_i and the cylinders are of the same material, the following equation gives the relation between the interference (difference in the diameters) and the interface pressure[1]:

$$\delta = \frac{4b^3(c^2-a^2)}{(b^2-a^2)(c^2-b^2)}\frac{p}{E} , \quad (1)$$

where δ is the interference between the two cylinders; p is the pressure between the two cylinders; E is Young's modulus of the material; and a, b, and c are the cylinder radii shown in Fig. 1.

For the usual geometries of subcells (inner cylinder) that are mounted in a common lens barrel (outer cylinder), the radii a, b, and c are approximately equal because the subcell and lens barrel are thin. Using the approximation $a \simeq b \simeq c$ in Eq. (1) gives

$$\delta = \frac{2pb^2}{E}\left(\frac{1}{t_o}+\frac{1}{t_i}\right) , \quad (2)$$

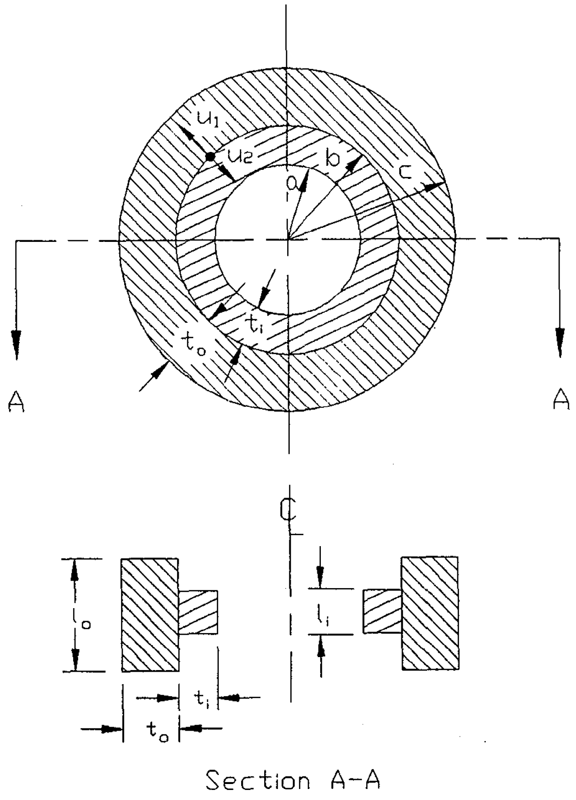

Fig. 1 Force-fitted cylinders to model a barrel lens mount.

where t_o and t_i are the thicknesses of the outer and inner cylinders, respectively. The radial displacement inward of the inner cylinder as shown in Fig. 1 is[1]

$$u_z = \frac{pb^2}{Et_i} . \tag{3}$$

Using Eq. (2), this radial displacement may be determined as a function of the interference fit, i.e.,

$$u_z = \left(\frac{\delta}{2}\right) \frac{t_o}{t_o + t_i} . \tag{4}$$

Equations (1) through (4) apply only when the inner cylinder is the same length as the outer cylinder. However, in barrel-mounted lenses the inner cylinder that represents the subcell is shorter than the barrel as shown in Fig. 1. To model this latter case, Eq. (4) is modified by introducing an *effective thickness* of the inner cylinder,

$$t_i^* = \beta t_i , \tag{5}$$

where β is an empirical function of l_o and l_i, which are the lengths of the outer and inner cylinders, respectively. Using finite element models of the two cylinder system of Fig. 1, the β function of Eq. (5) was found empirically to solve this axisymmetric elasticity problem:

$$\beta = 0.444 \left[1 - \frac{1}{2}\left(\frac{l_i}{l_o}\right) + \frac{7}{4}\left(\frac{l_i}{l_o}\right)^2 \right] . \tag{6}$$

2.1 *Subcell Strains, Stresses, and Displacements*

Shown in Fig. 2 is a typical barrel lens mount. It comprises a lens mounted in a metal ring using an elastomer annulus. This assembly is then force-fitted into the barrel tube. If Young's modulus of the elastomer is much less than those of the glass lens and the metal ring, the radial displacement at the outer boundary of the elastomer, u_r, is given by Eq. (4) modified by Eqs. (5) and (6):

$$u_r = \left(\frac{\delta}{2}\right) \frac{t_o}{t_o + t_i^*} . \tag{7}$$

The radial strain ε_r in the elastomer is[2]

$$\varepsilon_r = \frac{u_r}{t_e} , \tag{8}$$

where t_e is the radial thickness of the elastomer.

If the elastomer is thin relative to the lens edge thickness so that the elastomer is confined normal to the radial axis, the radial stress in the elastomer is[2]

$$\sigma_r = \frac{E_e \varepsilon_r}{1 + \nu_e} \left(1 + \frac{\nu_e}{1 - 2\nu_e} \right) , \tag{9}$$

where E_e is Young's modulus of the elastomer and ν_e is Poisson's ratio of the elastomer.

However, if the elastomer is not thin relative to the lens edge thickness so that the elastomer is confined only circumferentially, the radial stress in the elastomer is[2]

$$\sigma_r = \frac{E_e \varepsilon_r}{(1 - \nu_e^2)} . \tag{10}$$

Finite element analyses indicated in Eqs. (7), (8), and (9) are accurate for glass lenses mounted in metal rings with elastomers having a Young's modulus as high as 34.5 MPa. However, for stiffer elastomers, finite element analyses indicate that the empirical β function of Eq. (5) should be modified as follows:

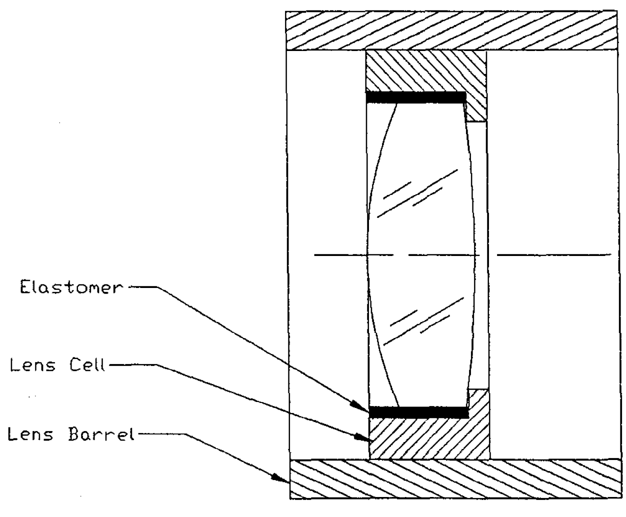

Fig. 2 A typical barrel lens mount.

$$\beta^* = \beta(1 + 7.83 \times 10^{-3} E_e) \ , \qquad (11)$$

where the modulus of the elastomer E_e is in units of megapascals.

The radial stress σ_r on the boundary of the lens is approximately equal to elastomer radial stress. It is this radial compressive lens stress that may be used to compute the optical path difference due to the glass stress.

2.2 *Verification Using Finite Element Modeling*

To verify the semiempirical formulation, finite element interference fit models were constructed using the GIFTS program.[3] Shown in Fig. 3 is one of the axisymmetric finite element models used. A lens is held in a mounting ring with epoxy and is then pressed into an outer ring. For this model the lens has a radius of 12.7 cm, a thickness of 2.54 cm, and the following material properties: $E = 6.9 \times 10^4$ MPa, $\nu = 0.17$. Both the inner and outer rings have the properties of steel ($E = 20.7 \times 10^4$ MPa, $\nu = 0.30$) and a thickness of 0.38 cm. The layer of epoxy has a thickness of 0.5 cm. This is a representative thickness recommended by manufacturers and suppliers of epoxies for optics of this size.

The factors that have the greatest influence on the stress induced by one of these mounting methods are the epoxy properties and the l_i/l_o ratio. To investigate the effects of the epoxy properties, a study was conducted where the diametrical interference and the l_i/l_o ratio were held constant. Young's modulus of the epoxy was varied from 3.45 to 345 MPa with a Poisson's ratio of 0.4. The results of this study are shown in Fig. 4. There is good agreement between the finite element results and the analytical solution when the Young's modulus of the epoxy is less than 10% of that of the mounting rings. It is also noted that the calculated stresses do not vary linearly with the Young's modulus of the epoxy.

The effects of varying the length of the mounting tubes (l_i/l_o) were also studied. As in the previous study, the diametrical interference was held constant as were the properties of the epoxy ($E = 3.45$ MPa, $\nu = 0.4$). The values for l_i/l_o were varied from 0.125 to 1 to obtain the results tabulated in Table 1. For all cases, there was good agreement between finite element and semiempirical solutions (less than 7% error). This study showed that changing the ratio of l_i/l_o had a lesser effect on the stresses than the impact of epoxy properties. Manufacturers and suppliers of elastomers are often unable or reluctant to specify the precise mechanical properties (E, ν, and G) of elastomers due to the variabilities that result from temperature, humidity, curing environment, etc. For this reason it is advisable to perform parametric studies using a range of expected mechanical properties to assess the effects of these variables on the optical performance of the lens.

2.3 *Optical Path Difference*

The stress induced in the glass when the lenses are mounted with an interference fit influences the refraction index of the lenses. The following relationship can be used to relate the optical path difference (OPD) due to the glass stress:

$$\Delta = K a \sigma \ , \qquad (12)$$

where K is the stress optical coefficient, a is the lens thickness (light path in medium), and σ is the tensile or compressive stress at the edge of the lens. If the lens is not of constant thickness, the stress, and therefore the OPD, will vary as the ratio of the edge thickness to the thickness at each point over the lens. This coefficient K, which is derived from the relationship between the effective stress and the OPD that results from stress-induced birefringence, is a material constant. This

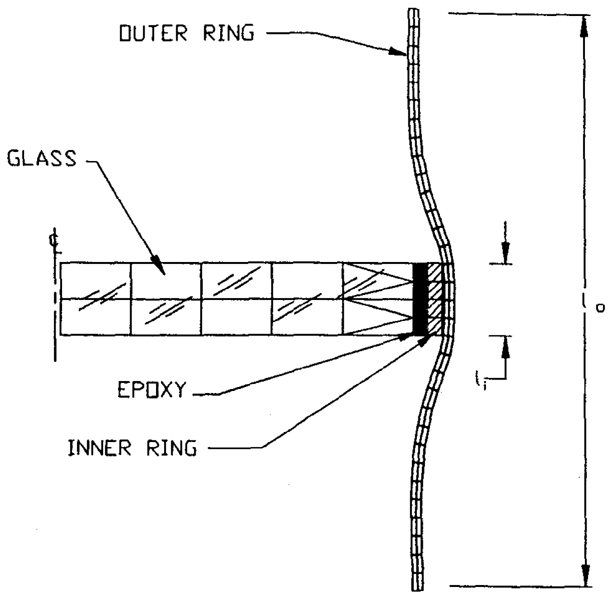

Fig. 3 Axisymmetric finite element interference fit model.

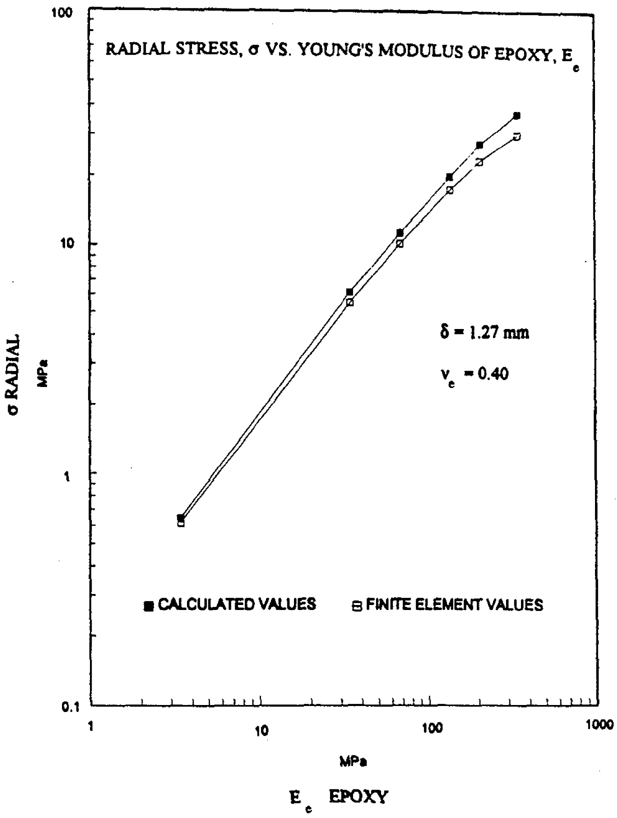

Fig. 4 Radial stresses for varying values of Young's modulus of the epoxy.

Table 1 Radial stress for varying tube length ratio (l_i/l_o).

δ = 1.27 mm		E_{Epoxy} = 3.45 MPa		ν = 0.40	
$\frac{l_i}{l_o}$	u radial (mm)	t_i* (eff)	σ radial (Eq. 9) (MPa)	σ radial(F.E.) (MPa)	Error between methods
0.125	0.442	1.63	0.6431	0.6123	5 %
0.167	0.442	1.63	0.6431	0.6116	5 %
0.250	0.439	1.65	0.6394	0.6019	6 %
0.500	0.414	1.98	0.6009	0.5716	5 %
1.00	0.315	3.81	0.4580	0.4309	6 %

stress optical coefficient of glass is typically determined from a uniaxial stress test. Equation (12) is a simplified approximation for this case; the stress optical coefficient for various glasses as well as a more detailed description of this formula can be found, for example, in the *Schott-Glass Catalog.*[4]

3 Decentration of Lenses

Decentration of lenses may be significant if the lenses are large and mounted in a relatively thick and compliant elastomer. The following analytical derivation for decentration may be used for gravitational, mechanical, and inertial lens loadings.

3.1 *Analytical Derivation*

To determine the decentration of lenses mounted in a circumferential flexible elastomer due to self-weight, consider the model of the tangent bar support system shown in Fig. 5. This model comprises six springs, three of equal stiffness k_r that act radially and three of equal stiffness k_t that act tangentially. For typical tangent bar designs the tangent spring constant is several orders of magnitude greater than the radial spring constant. Moreover, since the mirror or lens may usually be treated as a rigid body, the stiffness of the tangent bar support system in the plane normal to the optical axis is given by the following equation[5,6]:

$$K=\frac{3}{2}(k_r+k_t) \ , \tag{13}$$

where K is invariant, i.e., equal in all directions, in the plane of the support system.

If these springs are considered to have differential stiffness per unit length of $\bar{k}_r$ and $\bar{k}_t$ acting over a differential length of R dθ on the optical element boundary as shown in Fig. 6, the differential stiffness of this support system is

$$\mathrm{d}K=\frac{3}{2}(\bar{k}_r+\bar{k}_t)R \ \mathrm{d}\theta \ , \tag{14}$$

where R is the radius of the optical element.

For a continuous elastic support system, then,

$$K=\int_0^{\frac{2\pi}{3}} \frac{3}{2}(\bar{k}_r+\bar{k}_t)R \ \mathrm{d}\theta \ , \tag{15}$$

$$K=\pi R\,(\bar{k}_r+\bar{k}_t) \ , \tag{16}$$

where, for an elastomer, $\bar{k}_r$ is the extensional stiffness per unit length and $\bar{k}_t$ is the shear stiffness per unit length. When the elastomer thickness (radial) is approximately equal to the lens edge thickness, the elastomer may be modeled as a plane strain rectangular (quadrilateral) element. For a unit length,

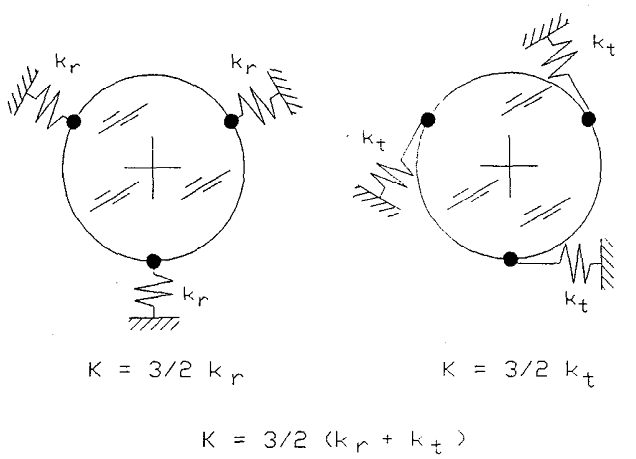

Fig. 5 Combined tangent bar support system.

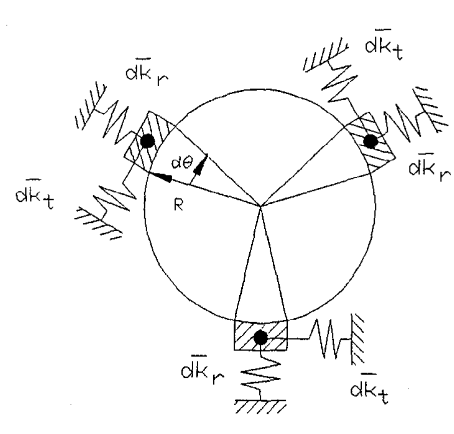

Fig. 6 Notation for analytical derivation.

$$\bar{k}_r = \left(\frac{E}{1-\nu^2}\right)\frac{d}{t_e} , \quad (17)$$

$$\bar{k}_t = G\frac{d}{t_e} , \quad (18)$$

where E is Young's modulus, G is the shear modulus, ν is Poisson's ratio, d is the optical element thickness, and t_e is the elastomer thickness (radial). The stiffness of the annulus of the elastomer is then

$$K = \pi R\frac{d}{t_e}\left(\frac{E}{1-\nu^2}+G\right) . \quad (19)$$

Decentering Δ of the optical element due to self-weight acting normal to the optical axis of the mirror may then be computed as follows:

$$\Delta = \frac{W}{K} , \quad (20)$$

where W is the weight of the optical element. Substituting for K,

$$\Delta = \frac{W}{\pi R\frac{d}{t_e}\left(\frac{E}{1-\nu^2}+G\right)} . \quad (21)$$

However, when the elastomer thickness (radial) is small compared to the lens edge thickness, the term $E/(1-\nu^2)$ in Eqs. (17), (19), and (21) should be replaced by $[E/(1+\nu)]\{1+[\nu/(1-2\nu)]\}$ to account for both tangential and radial elastomer confinement.

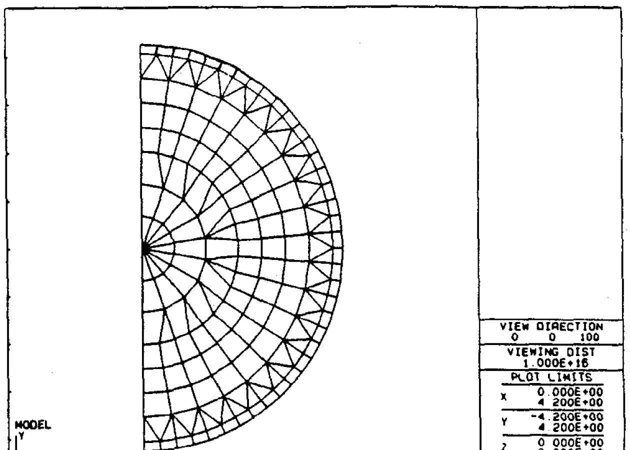

Fig. 7 GIFTS finite element model of a lens mounted in elastomer.

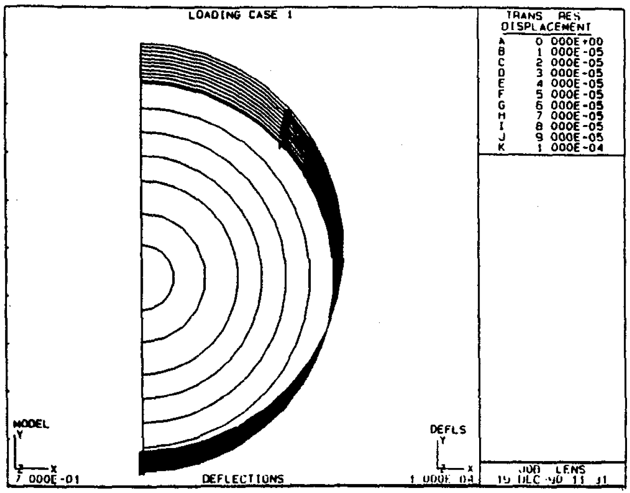

Fig. 8 Deflection of the lens model in the elastomer subject to lateral gravity loading.

3.2 *Verification of Finite Element Modeling*

To verify finite element solutions, models were constructed using the GIFTS program.[3] Shown in Figs. 7 and 8 is a 20.32-cm-diam lens with material properties of KZFSN9 glass. The first study used a lens of thickness 1.27 cm whereas the second study used a lens of 2.54 cm. In both cases the radial thickness of the elastomer was 0.51 cm. For the first case, the quadrilateral membrane elements were used as plane stress elements since the depth-to-thickness aspect ratio is 2.5. For the second case, these elements were used as plane strain elements since the depth-to-thickness ratio was 5.0. The results of this study are presented in Table 2 where the finite element solutions that use a low depth-to-thickness aspect ratio formulation for the thin lens and a high aspect ratio formulation for the thick lens are given. These analyses demonstrate the dominating influence of the mechanical properties of the elastomer, especially Poisson's ratio.

Acknowledgments

This work was performed under a contract with the U.S. Naval Observatory. The authors would also like to thank Daniel Vukobratovich for his helpful suggestions for this paper and Tina Guiney for her help with the illustrations.

References

1. C. T. Wang, *Applied Elasticity*, McGraw-Hill, New York (1953).
2. E. Volterra and J. H. Gaines, *Advanced Strength of Materials*, Prentice-Hall, New York (1971).
3. GIFTS-386, GIFTS version 6.5.1, CASA/GIFTS, Inc., Tucson, Arizona (May 1990).
4. *Schott-Glass Catalog*, Schott-Glass Technologies, Inc., 400 York Ave., Duryea, Penn. (1989).
5. R. M. Richard, M. Cho, and W. Pollard, "Dynamic analysis of the SIRTF one-meter mirror during launch," *Proc. SPIE* **973**, 86–99 (1988).
6. R. M. Richard, M. Cho, and W. Pollard, "The flexure assembly design for the SIRTF one-meter primary mirror," *Proc. SPIE* **973**, 79–85 (1988).

Table 2 Comparison of deflections for GIFTS and analytical solutions.

MATERIAL CONSTANTS		
Lens Material = KZFSN9		
E_{lens} = 6.600E4 MPa		
ν = 0.271		
Lens Radius = 10.16 cm		
Elastomer = 93-500 (DOW CORNING THIXOTROPIC)		
$E_{elastomer}$ = 3.45 MPa		
ν = 0.40		
Elastomer Thickness = .51 cm		
	CASE 1	**CASE 2**
Given		
Lens Tickness (cm)	1.27	2.54
Lens Weight (kg)	1.231	2.462
Δ (mm)		
Analytical Method	28.4E-3	2.05E-3
Gifts (FEM)	29.0E-3	1.80E-3

Tina M. Valente received a BS degree in mechanical engineering in 1987 from the University of Arizona. She is employed by the Optical Sciences Center at the University of Arizona where she is the leader of the optomechanics group. She has authored or coauthored 10 papers in the field of optomechanics.

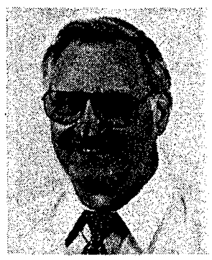

Ralph M. Richard is Professor Emeritus of Civil Engineering and Engineering Mechanics and is a Research Scientist in Optical Sciences at the University of Arizona. He has authored or coauthored more than 100 papers in the disciplines of structural and solid mechanics and optical structural engineering. He earned his BSCE from the University of Notre Dame, his MSCE from Washington University, and his PhD from Purdue University. He has been a consultant to the IBM Corporation, General Dynamics, NASA, and the Saudi Arabia Ministry of Communications.